Journal of Materials Chemistry C

ROYAL SOCIETY OF CHEMISTRY

PAPER

View Article Online
View Journal

Cite this: DOI: 10.1039/d6tc00697c

Designing adaptive materials for 3D-printing *via* dynamic covalent imine bonds

Marvin Kollwitz,[a] Jan Balszuweit,[a] Till Eisert,[a] Kateryna Loza[d] and Michael Giese *[abc]

Received 5th March 2026,
Accepted 29th April 2026

DOI: 10.1039/d6tc00697c

rsc.li/materials-c

A powerful platform for smart materials with adaptive surfaces enabling the post-processing tuning of the physical and mechanical properties is reported. More specifically, 3D-printed materials featuring dynamic covalent bonds at their surfaces are developed and tested with respect to their potential for dynamic property tuning. The integration of acrylates bearing amine groups into tailor-made resins enables post-printing modification of the surface by employing imine condensation or imine exchange reactions. This approach allowed the dynamic tuning of the surface polarity and fluorescence behavior of the 3D-printed objects. Furthermore, the application potential of this concept with respect to self-healable materials was demonstrated by employing the imine condensation reaction for dynamic-covalent welding.

1. Introduction

Additive manufacturing (AM), also known as 3D-printing, has developed into a transformative technology allowing facile and rapid processing of objects with complex shapes.[1] This advantage is particularly important in the biomedical,[2–4] construction,[5] energy[6] and aerospace[7] sectors for efficient production complex shapes. In the production of objects with complex architectures, the stereolithography techniques (SLA) such as digital light processing (DLP) have become established, as they have a resolution in the sub-micrometer range.[8] In the past, the focus was on optimizing the printing speed and improving the resolution. More recently, the synthesis of novel molecular building blocks in order to move from a conventionally 3D-printed material to 4D printing, providing additional features such as responsiveness or sensing capability, has gained more and more interest.[9–12] With respect to sustainable processing aspects such as self-healing capability or recyclability will play a crucial role.[13,14] The development of these materials requires the integration of responsive and adaptive components into the 3D-printed polymer matrix.[15]

The development of polymers that simultaneously exhibit self-healing and adhesive properties is highly desirable; however, it remains challenging, as these functionalities require inherently opposing bonding characteristics—dynamic, reversible interactions for self-healing and robust, stable interactions for effective adhesion. Although several self-healing elastomeric adhesives have been reported, the 3D-printability has only been established to a limited extent.[16–18] Adhering elastomer polymers often requires the use of adhesive additives. However, conventional adhesives often fail to establish a strong bond between materials and makes damages after removing or disassembly of the object. Here, dynamic covalent bonds (DCBs) represent a promising alternative to incorporate self-healing capability and adaptivity into a polymer. These bonds combine the ability of reversible network formation with the robustness of covalent bonds. The binders thus represent an added value regarding recyclability and adaptivity in the 3D printing sector.[19,20]

Recently, the work of Sowan *et al.* explored the use of dynamic covalent chemistry (DCC) at the resin silica-nanoparticle interface to enhance composite performance. Reversible covalent bonds at the interface enable efficient stress relaxation, which mitigates crack initiation and propagation. As a result, the composites exhibit significantly improved toughness under mechanical loading. The dynamic nature of the interfacial bonds, allowing damaged networks to recover structural integrity.[21] Moreover the work of Khairkkar *et al.* showed a method for adhesive-free bonding of incompatible polymer networks by dynamic covalent bond exchange at the interface. This creates a stable transition zone with high adhesive strength – even between stiff and soft or hydrophobic and hydrophilic materials. The method enables laminated hybrid structures without delamination and is suitable for applications in electronics, lightweight construction and coatings.[16] Wanasinghe *et al.* reported about the development of 3D-printable, self-healing elastomers that are incorporated into

[a] Organic Chemistry, University of Duisburg-Essen, Universitätsstraße 5-7, Essen 45141, Germany. E-mail: michael.giese@uni-due.de
[b] Co-Creation Lab Product Innovations, University of Duisburg-Essen, Schützenbahn 70, Essen 45127, Germany
[c] Center for Nanointegration Duisburg-Essen (CENIDE), Carl-Benz-Straße 199, 47057 Duisburg, Germany
[d] Inorganic Chemistry and Centre of Nanointegration Duisburg-Essen (CENIDE), University of Duisburg-Essen, Universitätsstr. 5-7 45141, Essen, Germany

the polymer network using thiol–Michael dynamics. In addition, acrylate monomers ensure strong adhesion to metallic and polymer surfaces. The resulting materials exhibit high elasticity (up to 2000%), self-healing performance of over 95%, and strong adhesion. They can process using a standard DLP 3D-printer and enable the printing of complex functional parts.[22]

In 2020 our group started to employed the dynamic nature of imine bonds to tune the properties of liquid crystalline (LC) materials.[23] By imine condensation, exchange or metathesis the nature of the mesophase, transition temperatures or emission behavior of the LC materials were post-synthetically adapted.[24]

Herein, we transfer our expertise in DCBs to develop dynamic-covalent materials for digital light processing (DLP) technologies. Our approach offers a versatile platform for dynamic surface design and material customization through controlled chemical exchange and thermal activation using dynamic covalent chemistry.

2. Results and discussion

2.1. Synthesis of adaptive material

A modular toolbox to develop new materials for DLP 3D-printing (see Fig. 1) containing (meth-) acrylate-based amines (see Fig. 1A) or aldehydes (see Fig. 1C) is presented to introduce reactive groups on the surface of the 3D-printed objects (research goal 1). These acrylates were added as dopants into established acrylate-based host resins. After processing *via* digital light processing (DLP) 3D-printing, the reactive amine groups on the surface were subsequently treated with a selection of aldehydes (see Fig. 1B) to form imines, allowing systematic tuning of the surface polarity and emission behavior of the materials (research goal 2). In addition, the introduction of the imine bonds provides the option for further post-synthetic manipulation of the material properties by imine exchange reactions (research goal 3). Finally, the potential of molecular welding of the materials *via* imine bond formation was investigated (research goal 4). Therefore, a second resin composition was designed featuring reactive aldehyde groups on the surface of the 3D-printed objects (see Fig. 1C).

2.1.1. Resin host system. In order to systematically address the scientific goals of the present study we initially focused on the identification of a suitable host resin ensuring compatibility of all component (host resin system as well as the functional monomers) in-turn with an efficient performance during 3D-printing process. It should be noted that most commercially available resin systems contain photo-stabilizers with strong auto-emission, which make them unsuitable in the present study due to interference with the emission behavior of the salicyl-imines and the concept of emission tuning *via* dynamic

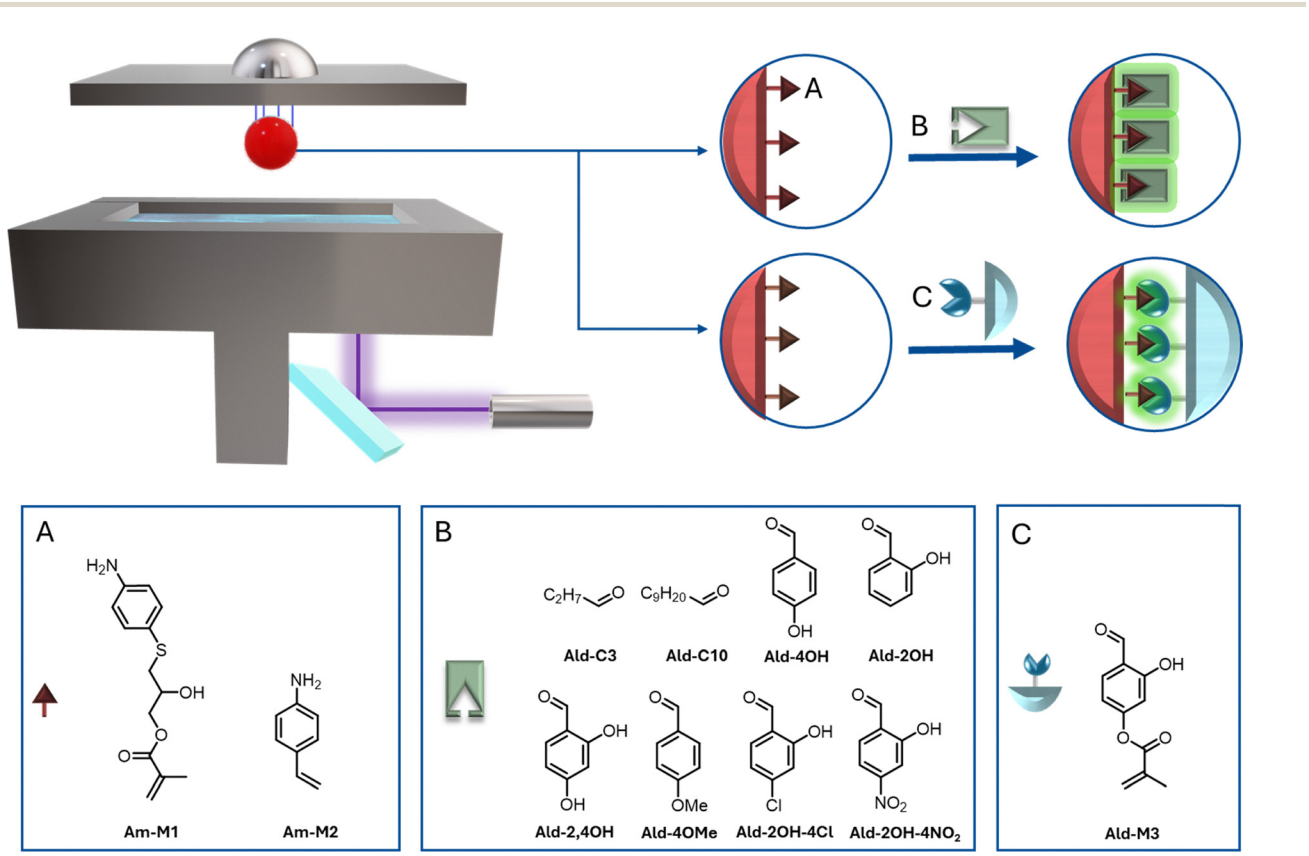

Fig. 1 Schematic representation of the DLP 3D printing process (upper left) and the manipulation of the materials properties by imine condensation and exchange reactions on the materials' surface (upper right). (A) represents the self-synthesised amine monomer **Am-M1** and commercially available **Am-M2**, (B) used aldehyde derivatives for modification of contact angle and photoluminescence emission. C) representation of self-synthesised aldehyde monomer **Ald-M3** and corresponding polymer **P3** for welding experiments.

condensation and exchange reactions. Therefore, a custom-made resin system had to be developed. Systematic variations of the formulation of the host resin yielded the custom-made photopolymer **P0**, containing 2-[[(butylamino)-carbonyl]oxy]-ethyl acrylate (2BAEA, 94 wt%) as main component, poly-(ethylene glycol)-dimethacrylate (PEGDMA, Mn ~750 g mol^{-1}, 5 wt%) to introduce flexibility and diphenyl-(2,4,6-trimethyl-benzoyl)-phosphine oxide (TPO, 1 wt%) as photo-initiator. This host system combines mechanically robustness with elasticity (see Table S1) as reliable platform for chemical modifications.

2.1.2. Acrylates with reactive groups. The host system **P0** was doped with 2 wt% of self-synthesized **Am-M1** or commercially available **Am-M2** (see Fig. 1A and Fig. S2 and S3) to introduce amine-groups into the polymer systems for subsequent modification of the materials surface *via* dynamic-covalent condensation and exchange reactions (yielding polymer compositions **P1** and **P2**, all details on the development of the resin system as well on the characterisation of the printing behavior can be found in the supporting material Fig. S7–S13). It should be noted that resin formulations with higher amounts of **Am-M1** and **Am-M2** yielded precipitation, thus in the following only the formulations with 2 wt% of the amine-bearing monomers have been used. The successful printing test yielded 3-dimensional objects with uniform distribution of amine groups on the surface as determined by FT-IR, SEM-EDX, fluorescence emission and contact angle measurements.

The successful printing of the developed resins yielded 3-dimensional objects (see Fig. 2) bearing either aldehyde or amine groups on their surface, which were used in the following for modification of the material properties by imine condensation reactions.

For the investigation of the welding potential **Ald-M3**, based on 2,4-dihydroxybenzaldehyde, was synthesized as an additional functional monomer. The *ortho*-phenolic hydroxyl group serves as functional group for the formation of highly emissive salicyl imines, while the *para*-hydroxy group offers a reactive site for the derivatization, such as the conversion into the corresponding methacrylate **Ald-M3** (see Fig. S5 and S6 for NMR characterization). The functional monomer **Ald-M3** was added to **P0** (2 wt%), processed *via* DLP 3D-printing and the resulting specimen was combined with amine-functionalized 3D-printed structures to investigate the welding performance.

2.2. Analysis of surface functionalization

The surface topology and chemical functionalization of the polymers were investigated by SEM–EDX measurements. The image of the lateral view of the fabricated material shows the characteristic layers of the 3D-printed structure with a layer thickness of ~100 µm, as expected (see Fig. 3A). In addition, SEM images of the surface of the 3D-printed samples were obtained before (**P2**) and after functionalization (**P2-Cl**) with imines, which clearly show no impact on the topology by the functionalization (see Fig. 3B and C). Similar results were found for the surfaces of **P1** and **P1-Cl** (see Fig. S30 and S31).

In order to proof the surface functionalization of the materials EDX analysis before and after imine condensation was performed (see Fig. 3D). As an indicator for successful functionalization the chlorine content at the surface was used, which was introduced by imine condensation between the amine functionalized surface and 4-chloro-2-hydroxybenzaldehyde (**Ald-2OH-4Cl**). The EDX analysis of the custom-made host resin **P0** reveals carbon, oxygen, and nitrogen contents of 55%, 40%, and %, respectively (see Table 1). Comparable elemental compositions were obtained for **P1** (which contains 2 wt% of the amine monomers **Am-M1**). As shown in Table 1, **P2**, which contains 2 wt% of the monomer **Am-M2**, shows an increased nitrogen content, which can be attributed to the lower molecular weight of **Am-M2** and thus a higher molar ratio given that

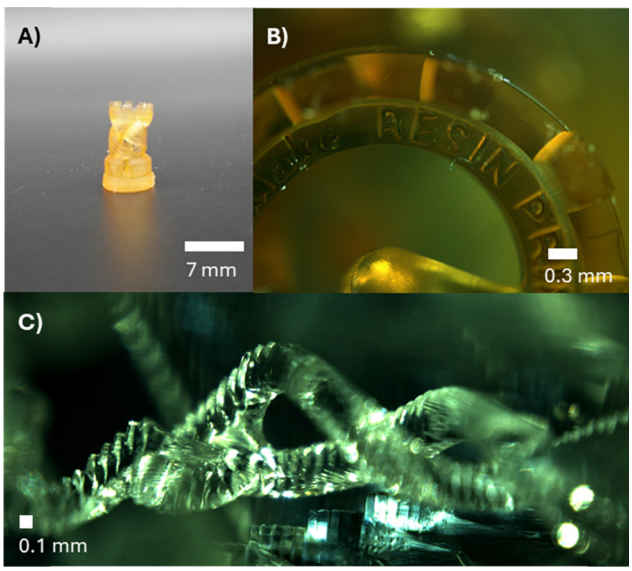

Fig. 2 3D-printed structure of **P1** (A), including macroscopic images of the letters on the surface (B) and the internal helical structures (C).

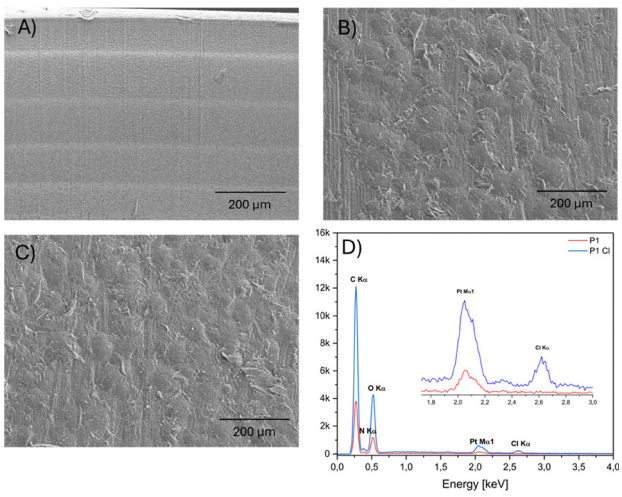

Fig. 3 SEM images of the lateral view of the 3D-printed layer by layer structure of **P0** (A), surface topology of unfunctionalized (B) and functionalized (C) samples of **P2** and **P2-Cl** coated with 4-chloro-2-hydroxynbenzaldehyde (**Ald-2OH-4Cl**). EDX analysis of **P1** and **P1-Cl** with signal comparison and newly formed detectable chlorine signal at 2.6 keV.

Table 1 Quantitative EDX elemental composition data for polymers **P0**, **P1**, **P1-Cl**, **P2** and **P2-Cl**. Polymers **P1** contain 2 wt% of **Am-M1** and **P2** contain 2 wt% of **Am-M2**

Elements	Weight % **P0**	Weight % **P1**	Weight % **P1-Cl**	Weight % **P2**	Weight % **P2-Cl**
C	55.3	54.7	52.0	50.7	53.0
O	39.9	40.0	38.9	37.9	35.4
N	4.7	5.3	7.7	11.5	9.4
Cl	—	—	1.4	—	1.2

the addition of the functional monomers is provided in weight percent. Consequently, the overall nitrogen contribution is increased. Upon functionalization of the 3D-printed objects with **Ald-2OH-4Cl** the chlorine content at the surface of the materials was studied by SEM–EDX analysis. As expected **P1** and **P2** showed no detectable amount of chlorine at the surface (see Table 1). In contrast, after functionalization with **Ald-2OH-4Cl** a signal for chlorine was observed. In detail, a chlorine content of 1.4 wt% for **P1-Cl** and 1.2 wt% for **P2-Cl** were detected, providing evidence for successful surface functionalization with chlorine-containing imines.

2.3. Tuning the surface polarity

Numerous strategies have been reported for tailoring the polarity of surfaces *via* chemical post-functionalization, including thiol-Michael addition, Staudinger–Vilarrasa reaction or Huisgen cycloaddition.[25–28] While these approaches are highly efficient, they typically result in lack of the formation of reversible bonds. In contrast, the use of dynamic covalent chemistry (DCC) offers the advantage for the design of adaptive or ''smart'' surfaces and materials.[29–31] Due to the reversibility of imine bond formation, surfaces with adjustable properties—such as controlled and reversible adjustments to surface polarity, emission behavior, and weldability—can integrated. Furthermore, we investigated the ability of the 3D-printed materials to tune the polarity of the surface by imine condensation. Therefore, the 3D-printed objects were placed in 0.01 M solution of the corresponding aldehyde in methanol (~2 mL) for 5 min. After color change, the samples were removed from the solution and dried for 15 min at ambient conditions. Surface functionalization was confirmed by FT-IR spectroscopy (Fig. S14 and S15). For the nomenclature of the samples the following system is employed. For example, the 3D-printed sample from **P1** treated with 4-hydroxybenzaldehyde (**Ald-4OH**) turns into the corresponding imine labeled as **Im4OH@P1**. For materials covered with propionaldehyde the imine labeled as **ImC3@P1**, decanal **ImC10@P1**, 4-methoxybenzaldehyde **Im4OMe@P1**, 2,4-dihydroxybenzaldehyde **Im2,4OH@P1**, 2-hydroxybenzaldehyde **Im2OH@P1**, 4-chloro-2-hydroxybenzaldehyde **Im4ClSalAld@P1**, 4-nitro-2-hydroxy-benzaldehyde **Im4NO$_2$SalAld@P1**. For polymer **P2** the same nomenclature was selected as imine **Im4OH@P2** was functionalized with 4-hydroxybenzaldehyde and **ImC3@P2**, **ImC10@P2**, **Im4OMe@P2**, **Im2,4OH@P2**, **Im2OH@P2**, **Im4ClSalAld@P2**, **Im4NO$_2$SalAld@P2**.

After preparing the imine functionalized materials, contact-angle measurements were conducted to investigate the wetting behavior with respect to water droplets. In general, contact angles can be classified into two categories: surfaces with contact angles below 90° are considered hydrophilic, whereas those above 90° are regarded as hydrophobic. Samples printed with the unmodified host resin **P0** showed a contact angle of 87°, while **P1** exhibited a contact angle of ~85° and **P2** an angle of 91°, respectively. These values indicate slight changes in the polarity after introduction of the amine monomer. Upon imine condensation at the surface of **P1** contact angles between 80° and 100° were obtained (see Fig. S16 and S18), while the reaction of propionaldehyde yielded the highest value of ~100° and 4-nitro-2-hydroxybenzaldehyde the lowest with 80°. Notably, the contact angle obtained for the imine by decanal did not exceed that of the C3 analogue. This effect may arise from steric and packing effects at the interface, where excessive molecular crowding can induce lateral repulsion, thereby hinder uniform surface coverage and limiting further increases in hydrophobicity.[32]

The imine condensation at the surface of **P2** led to similar result with contact angles between 66° and 95° (see Fig. S17 and S19), indicating predominantly hydrophobic characteristics of the surface. Interestingly, the presence of polar terminal groups does not appear to significantly affect the contact angle. For instance, the imine derived from 2,4-dihydroxybenzaldehyde exhibits a contact angle of 93°, comparable to that of the imine containing 4-methoxybenzaldehyde, despite the substantially higher polarity expected for the dihydroxy substituents. It was found that the system does not exhibit any significant change in surface polarity even when polar aldehyde systems are applied.

To harness the potential of dynamic covalent chemistry for surface functionalization, an exchange reaction at the surface of an imine-functionalized polymer was performed to tune the polarity of the surface. As a representative example **P1** decorated with **Im4OH** (**Im4OH@P1**) was treated with 4-nitro-2-hydroxybenzaldehyde (**Ald-2OH-4NO$_2$**), since for this exchange reaction the strongest shift in the surface polarity is expected. Initially the surface of **Im4OH@P1** was found to be slightly hydrophobic with a contact angle of 99° (see Fig. 4). However, after treating the surface with a solution of **Ald-2OH-4NO$_2$** in methanol for 2 hours the contact angle significantly decreased to 79°, indicating an increase in the polarity of the surface induced by the successful exchange of **Im4OH**.

These initial results show that imine condensation on the surface of **P1** and **P2** enables the manipulation of the surface polarity. However, the differences in the contact angles and thus in the surface polarity are less pronounces as expected, which might be attributed to the low density of functional groups on the surfaces of the 3D-printed materials. In this context the tuning of the emission behavior of the materials is a promising target, since already the presence of a small amount of a luminophore will have a significant impact on the fluorescence properties.

2.4. Tuning the emission properties

The second property of the materials which was tuned *via* imine condensation and exchange reaction was the emission

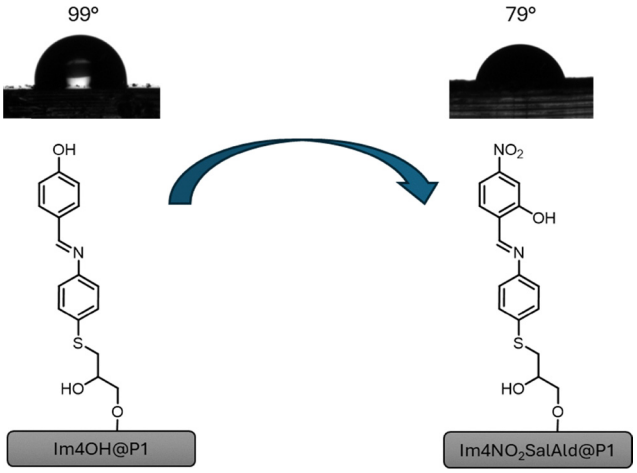

Fig. 4 General concept for switching surface wettability with dynamic covalent chemistry. Left contact angle of **Im4OH@P1** with 99° and right after exchange **Im4NO$_2$SalAld@P1** and contact angle of 79°.

behavior. Dynamic covalent chemistry is now employed in diverse chemical disciplines, spanning the creation of molecular and bulk self-assembled materials as well as the design of fluorescent sensors and artificial molecular machines. Therefore, the surface-functionalized 3D-printed objects with amine-groups (**P1** and **P2**) were treated with 0.01 M solutions of aldehydes (see listed aldehydes above) in methanol and subsequently investigated with respect to their emission behavior. The untreated samples showed emission maxima at 517 and 518 nm for **P1** and **P2**, respectively, with a low relative intensity caused by the fluorescence of the amine components (S20, S21, S22, S23, S24 and S25).[33–35] Upon treatment with aldehydes, the emission wavelengths show a hypsochromic shift from 517 nm to ~470 nm for aliphatic imines (C3 and C10), while the aromatic imines yield a bathochromic shift of the emission wavelength to 533–576 nm, depending on the electronic nature of the aromatic imine. The most pronounced bathochromic shift was found for **ImNO$_2$SalAld@P1** with an emission wavelength maximum at 576 nm. The significant bathochromic shift can be explained by the electron-deficient character of the nitro-arene enhancing the push–pull character of the emissive imine.[36–38] This is in-line with the general trend of the bathochromic within the series of investigated imines. In contrast, the imines with an alkyl rest show a hypsochromic shift which is caused by the reduction of the push–pull character due to the electronic nature of the alkyl chains.[39–41] The treatment of **P2** with aldehydes to form imines on the surface of the 3D-printed samples produced results comparable to those obtained for the **P1** surface modification (see Fig. S23). These findings suggest that the fluorescence properties of the materials can readily be modulated through simple treatment of the surface after 3D-processing. In order to harvest the full potential of the dynamic-covalent imine bond, the emission properties of the surface-functionalized materials were tuned by imine exchange reaction.

2.5. Tune emission properties *via* DCC exchange reaction

Imines are well known to undergo exchange reactions with aldehydes to form a new imine and release of an aldehyde.[42,43] In order to tune the fluorescence behavior of the 3D-printed objects a sample of **ImC3@P1** was prepared, showing an emission maximum at 471 nm. Upon treatment of this sample with **Ald-2OH-4NO$_2$** a hypsochromic shift occurs by shifting the emission maximum from 471 nm to 576 nm, while a color change from blue to orange is recognizable by eye. This color change is in-line with the expected emission behavior when transforming from **ImC3@P1** to **ImNO$_2$SalAld@P1**, indicating successful exchange of the imine bond (see Fig. 5) at the surface of the 3D-printed sample.

In order to tune the fluorescence properties of material **P2** we explored a cascade reaction of the imine modified polymer with **Ald-2OH-4Cl** to achieve a greenish fluorescence and further modification with **Ald-2OH-4NO$_2$** yield to an emission in the yellowish area at around 580 nm (see Fig. 6).

2.6. Material welding by DCC

The previous results clearly demonstrate the potential of the dynamic-covalent bonds for tuning the properties of the materials surface, namely the wettability and the fluorescence behavior. In a next step we were curious if the amine groups on the surface can be employed for dynamic-covalent ''welding''. Therefore, the library of 3D-printable resin systems was extended by **P3**, which contains **Ald-M3** as aldehyde counterpart to the amine-acrylate containing resins **P1** and **P2**. The 3D-printed samples with amine groups on the surface **P1** or **P2** were combined with an object surface-functionalized with aldehyde moieties (**P3**, details see Fig. S27) and tested with respect to their mechanical properties. As reference the mechanical properties of **P0** (resin system without dopant), **P1**, **P2** (amine-doped resins) and **P3** (aldehyde doped resin) were investigated by tensile tests. For the mechanical properties of the 3D-printed parts, rectangular tensile bars with a length of 75 mm, a width of 5 mm, and a thickness of 2 mm were printed. After printing, samples were

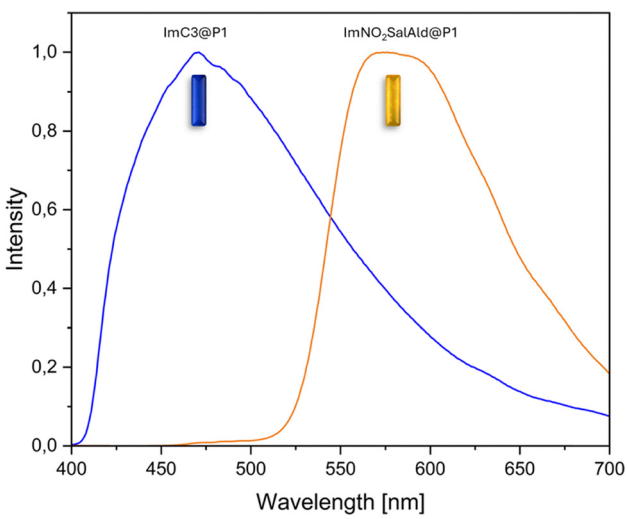

Fig. 5 Emission spectra and photograph of the samples upon exchange reaction at surface **ImC3@P1** (blue curve) with 4-nitro-2-hydroxybenzimine (orange curve). Excitation with 395 nm.

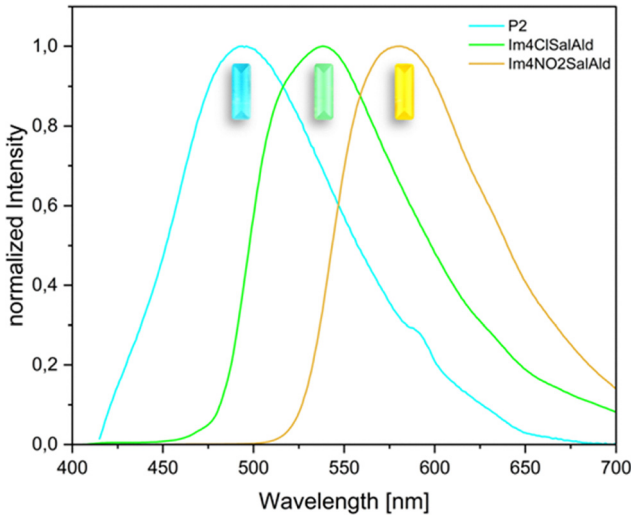

Fig. 6 Emission spectra and photograph of the cascade reaction of **P2** (blue line) starting from 4-Chloro-2-hydroxybenzimine (green line) towards the functionalization of the surface with 4-Nitro-2-hydroxybenzimine (orange line) *via* exchange reaction.

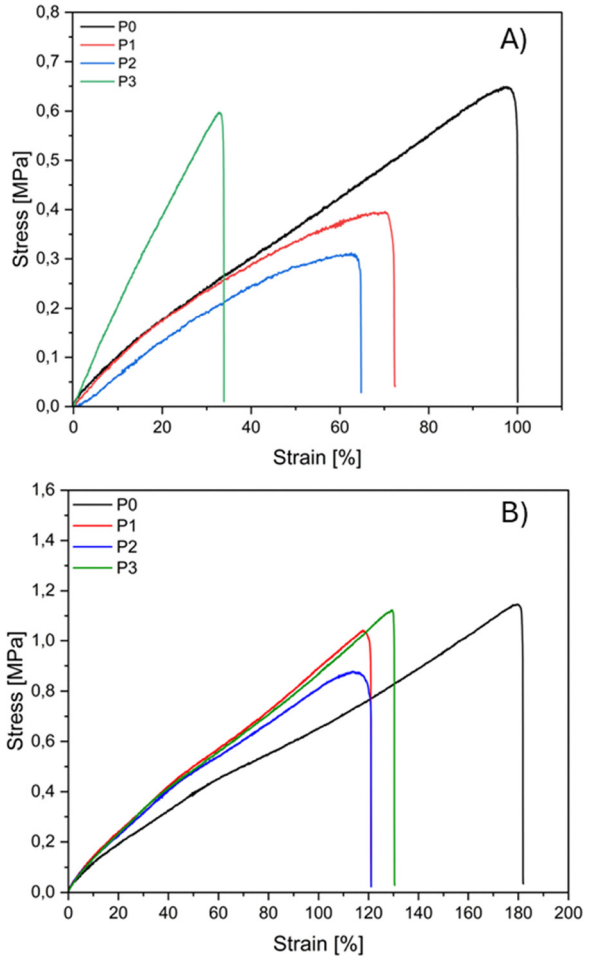

Fig. 7 Tensile tests of polymers **P0**, **P1**, **P2**, and **P3** at room temperature (A), and after annealing at 80 °C for 24 h in an oven (B). Tests were performed at room temperature at a crosshead speed of 25 mm min^{-1}.

washed in isopropanol (IPA) for 5 minutes, air-dried for 10 minutes and post-cured for 4 minutes at room temperature.

The stress–strain diagrams of the reference measurements (pristine polymer samples without weld seam) show that the ultimate tensile stress decreases with addition of **Am-M1** and **Am-M-2** from 0.65 MPa (**P0**), 0.39 MPa (**P1**) and 0.32 MPa (**P2**), respectively (see Fig. 7a). The reduction in mechanical strength might be attributed to differences in the reaction kinetics of the monomers **Am-M1** and **Am-M2** compared to 2-[[(butylamino)-carbonyl]oxy]ethyl acrylate (2BAEA), which yields an increase of the internal stress and in turn reduction of the mechanical strength.[44,45] This assumption is supported by the elongation results: **P0** shows an elongation of 98%, **P1** of 72%, and **P2** of 65%. In contrast, the tensile strength of polymer samples with **Ald-M3** (**P3**) was comparable to 0.6 MPa the initial tensile strength of **P0**, however, the elongation is reduced to 33% (see Fig. 7).[46,47]

For the welding experiments the sample design was optimized with complementary shapes (see Fig. S27). Subsequently, the amine (**P1** or **P2**, Fig. S27 top part) component and the aldehyde bottom counterpart (**P3**) were precisely overlapped and kept together under a constant compressive load of 1 N for 10 minutes. Since the imine bond formation yields a change in the emission behavior of the materials, the bond formation can be followed by fluorescence spectroscopy. While **P1**, **P2** and **P3** shows fluorescence signals at 517 nm, 518 nm and 455 nm, respectively, the newly formed imine between the interface of the samples exhibit a signal at 537 nm for **P1–P3** and 545 nm for **P2–P3** (see Fig. 8 and Fig. S29). This shift in the fluorescence behavior can be followed by the naked eye (see Fig. 8B), which provides a simple method to follow the welding process.

The welding process was finalized by thermal curing of the samples at 80 °C for 24 h. Heating facilitates the formation of dynamic covalent bonds by promoting the removal of water produced during the condensation between aldehyde and amine groups. This approach has been previously demonstrated to be effective in bulk imine formation for the synthesis of imine-based liquid crystals.[23,24] It should be noted that after heating polymer **P2** at 80 °C for 48 h, the material exhibited slight surface defects but no evidence of structural degradation. As shown in Fig. S28, FT-IR data confirms the presence of residual polymerization. The stress–strain measurements of the welding samples of **P1–P3** and **P2–P3** exhibited comparable ultimate tensile stress of ~0.2 MPa after one day in oven at 80 °C (Fig. 9). However, since the welding process is based on the formation of dynamic-covalent imine bonds formation, we examined the influence of surface functionalization density by increasing the aldehyde functionality in the **P3** formulation to twofold (4 wt% **Ald-M3**) and tenfold (10 wt% **Ald-M3**) the initial aldehyde monomer concentration.

For the sample series **P2–P3** the mechanical properties are affected with an increase in the stress strength from 0.18 ± 0.05 MPa (**P2–P3**), to 0.33 ± 0.17 MPa (**P2–P3x2**) to 0.55 ± 0.07 MPa MPa (**P2–P3x10**). The elongation remained nearly unchanged in this series at around 60%. The most

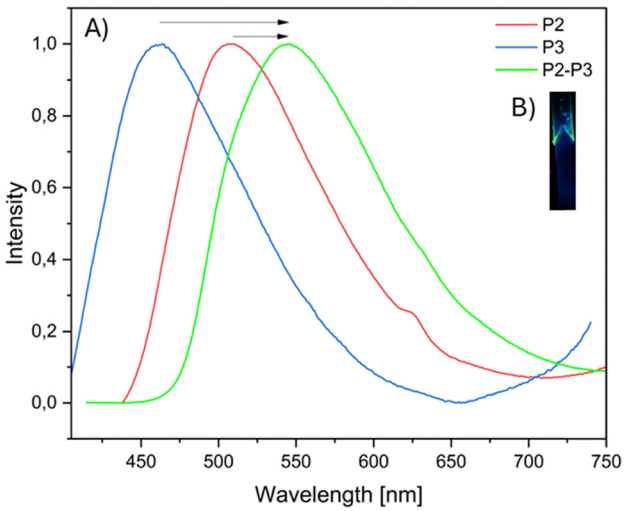

Fig. 8 (A) Emission spectra of polymers **P2** (red curve) and **P3** (blue curve), as well as of the interracially welded sample **P2–P3** (green curve). (B) Photograph showing the emission at the **P2–P3** interface under UV irradiation of 395 nm.

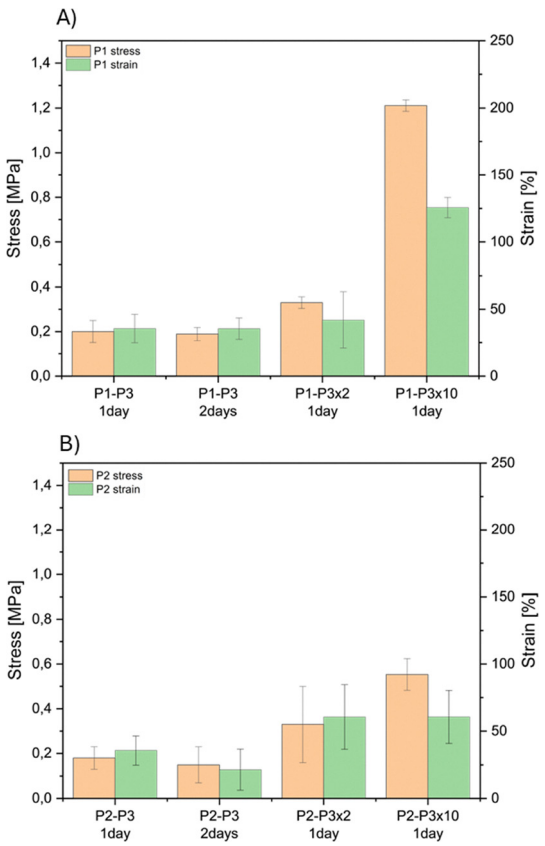

Fig. 9 Tensile properties of welded samples **P1–P3** (A) and **P2–P3** (B). The bar charts present the ultimate tensile strength (orange bars, left *y*-axis) and the corresponding elongation at break (green bars, right *y*-axis) for samples treated at 80 °C for different durations (1–2 days) and with varying **Ald-M3** contents (P3 (2 wt% **Ald-M3**), P3 × 2 (4 wt% **Ald-M3**), P3 × 10 (20 wt% **Ald-M3**)).

pronounced improvement in mechanical strength was observed for the **P1–P3x10** system treated at 80 °C for 24 h. The tensile strength increased by approx six-fold compared to the initial condition (**P1–P3**) from 0.2 MPa to 1.2 MPa.

The stress–strain measurements of the welded samples demonstrate that the thermal curing time (24 *vs.* 48 h) and temperature (80 *vs.* 100 °C) only has a small effect on the mechanical behavior of the samples. In contrast, the increase of the density of functional groups on the surface of the leads to a significant improvement of the mechanical robustness of the samples.

3. Conclusion

In conclusion, we report a modular approach towards 3D-printable materials featuring dynamic covalent bonds on the surface, allowing the tuning of the surface properties by making use of imine condensation and exchange reactions. Therefore, a series of acrylates bearing peripheral amine groups was synthesized and embedded in custom-made resins for digital light processing 3D-printing. Subsequently to the 3D-printing process the amine groups were used in imine condensation to tune the surface polarity. Due to the relatively low amount (2 wt%) of acrylates with amine groups the impact of the surface polarity was small, reflected by a change of the contact angle from 85° for **P1** to 91° for **P2**.

However, the emission behavior of the materials could be significantly and dynamically be tuned from 517 to 540 and 581 nm. Beside the changes in the polarity and the photophysical properties the surface modification *via* dynamic covalent chemistry was followed by FT-IR and SEM-EDX measurements. As a proof-of-concept the imine condensation was used in a dynamic-covalent welding approach. Therefore, an additional acrylate was synthesized and added to the custom-made resin composition. These materials act with its aldehyde groups as dynamic-covalent counterpart to the amine-functionalized samples and by imine condensation between the two different surfaces the imine formation yielded dynamic-covalently welded specimens, which showed an increased tensile strength by ∼six-fold from 0.2 MPa to 1.2 MPa compared to the initial condition.

This work presents a robust strategy for dynamically tuning both mechanical and optical properties of polymeric materials. The results demonstrate a versatile approach to creating reprogrammable, responsive surfaces and modular polymeric devices. This study sets the foundation for future developments in smart materials, adaptive interfaces, and multifunctional systems, where control over surface chemistry, mechanics, and fluorescence is required by dynamic covalent chemistry.

Author contributions

The manuscript was written through contributions of all authors. All authors have given approval to the final version of the manuscript.

Conflicts of interest

The authors declare no competing financial interest.

Data availability

The data supporting this article have been included in the supplementary information (SI). Supplementary information is available. See DOI: https://doi.org/10.1039/d6tc00697c.

Acknowledgements

We thank all collaborators who are involved in this project. Especially Dr Jan Balszuweit and Till Eisert for synthetic work and Dr Kateryna Loza for the SEM-EDX measurements. The authors M. K. and M. G. gratefully acknowledge funding from DFG Heisenberg-Program (project number 443479537).

References

1 S. Park, W. Shou, L. Makatura, W. Matusik and K. Fu, 3D printing of polymer composites: Materials, processes, and applications, *Matter*, 2022, **5**, 43–76, DOI: 10.1016/j.matt.2021.10.018.
2 S. V. Murphy and A. Atala, 3D bioprinting of tissues and organs, *Nat. Biotechnol.*, 2014, **32**, 773–785, DOI: 10.1038/nbt.2958.
3 W. Zhu, X. Ma, M. Gou, D. Mei, K. Zhang and S. Chen, 3D printing of functional biomaterials for tissue engineering, *Curr. Opin. Biotechnol.*, 2016, **40**, 103–112, DOI: 10.1016/j.copbio.2016.03.014.
4 Q. Yan, H. Dong, J. Su, J. Han, B. Song, Q. Wei and Y. Shi, A; Review of 3D Printing Technology for Medical Applications, *Engineering*, 2018, **4**, 729–742, DOI: 10.1016/j.eng.2018.07.021.
5 Y. W. D. Tay, B. Panda, S. C. Paul, N. A. Noor Mohamed, M. J. Tan and K. F. Leong, 3D printing trends in building and construction industry: a review, *Virtual Phys. Prototyping*, 2017, **12**, 261–276, DOI: 10.1080/17452759.2017.1326724.
6 M. P. Browne, E. Redondo and M. Pumera, 3D Printing for Electrochemical Energy Applications, *Chem. Rev.*, 2020, **120**, 2783–2810, DOI: 10.1021/acs.chemrev.9b00783.
7 S. C. Joshi and A. A. Sheikh, 3D printing in aerospace and its long-term sustainability, *Virtual Phys. Prototyping*, 2015, **10**, 175–185, DOI: 10.1080/17452759.2015.1111519.
8 A. Vedhanayagam, M. Golfetto, J. L. Ram and A. S. Basu, Rapid Micromolding of Sub-100 μm Microfluidic Channels Using an 8K Stereolithographic Resin 3D Printer, *Micromachines*, 2023, **14**, 1519, DOI: 10.3390/mi14081519.
9 R. Sajjad, S. T. Chauhdary, M. T. Anwar, A. Zahid, A. A. Khosa, M. Imran and M. H. Sajjad, A review of 4D printing – Technologies, shape shifting, smart polymer based materials, and biomedical applications, *Adv. Ind. Eng. Polym. Res.*, 2024, **7**, 20–36, DOI: 10.1016/j.aiepr.2023.08.002.
10 X. Kuang, D. J. Roach, J. Wu, C. M. Hamel, Z. Ding, T. Wang, M. L. Dunn and H. J. Qi, Advances in 4D Printing: Materials and Applications, *Adv. Funct. Mater.*, 2019, **29**, 1805290, DOI: 10.1002/adfm.201805290.
11 A. S. Gladman, E. A. Matsumoto, R. G. Nuzzo, L. Mahadevan and J. A. Lewis, Biomimetic 4D printing, *Nat. Mater.*, 2016, **15**, 413–418, DOI: 10.1038/nmat4544.
12 D.-G. Shin, T.-H. Kim and D.-E. Kim, Review of 4D printing materials and their properties, *Int. J. Precis. Eng. Manuf. Green Technol.*, 2017, **4**, 349–357, DOI: 10.1007/s40684-017-0040-z.
13 B. Arsuffi, T. Magrini, M. Champeau, G. Siqueira and S. Titotto, 4D printing of natural materials: A review, *Sustainable Mater. Technol.*, 2025, **44**, e01346, DOI: 10.1016/j.susmat.2025.e01346.
14 G. Zhu, H. A. Houck, C. A. Spiegel, C. Selhuber-Unkel, Y. Hou and E. Blasco, Introducing Dynamic Bonds in Light-based 3D Printing, *Adv. Funct. Mater.*, 2024, **34**, 2300456, DOI: 10.1002/adfm.202300456.
15 B. Narupai and A. Nelson, 100th Anniversary of Macromolecular Science Viewpoint: Macromolecular Materials for Additive Manufacturing, *ACS Macro Lett.*, 2020, **9**, 627–638, DOI: 10.1021/acsmacrolett.0c00200.
16 S. Khairkkar, A. V. Pansare, S. V. Pansare, S. Y. Chhatre, J. Sakamoto, M. Barbezat, G. P. Terrasi, V. R. Patil, A. A. Nagarkar and M. Naito, Adhesive-less bonding of incompatible thermosetting materials, *RSC Appl. Polym.*, 2025, **3**, 247–256, DOI: 10.1039/d4lp00288a.
17 G. Bovone, O. Y. Dudaryeva, B. Marco-Dufort and M. W. Tibbitt, Engineering Hydrogel Adhesion for Biomedical Applications via Chemical Design of the Junction, *ACS Biomater. Sci. Eng.*, 2021, **7**, 4048–4076, DOI: 10.1021/acsbiomaterials.0c01677.7.
18 G. Raos and B. Zappone, Polymer Adhesion: Seeking New Solutions for an Old Problem, *Macromolecules*, 2021, **54**, 10617–10644, DOI: 10.1021/acs.macromol.1c01182.
19 L. L. Robinson, J. L. Self, A. D. Fusi, M. W. Bates, J. Read de Alaniz, C. J. Hawker, C. M. Bates and C. S. Sample, Chemical and Mechanical Tunability of 3D-Printed Dynamic Covalent Networks Based on Boronate Esters, *ACS Macro Lett.*, 2021, **10**, 857–863, DOI: 10.1021/acsmacrolett.1c00257.
20 Y. Jia, C. A. Spiegel, J. Diehm, D. Zimmermann, B. Huber, H. Mutlu, M. Franzreb, M. Wilhelm, P. Théato, E. Blasco and M. Tsotsalas, Investigating Dynamic Changes in 3D-Printed Covalent Adaptable Polymer Networks, *Macromol. Mater. Eng.*, 2024, **309**, 2300438, DOI: 10.1002/mame.202300438.
21 N. Sowan, C. N. Bowman, L. M. Cox, P. K. Shah, H. B. Song and J. W. Stansbury, Dynamic Covalent Chemistry at Interfaces: Development of Tougher, Healable Composites through Stress Relaxation at the Resin-Silica Nanoparticles Interface, *Adv. Mater. Interfaces*, 2018, **5**, 1800511, DOI: 10.1002/admi.201800511.
22 S. V. Wanasinghe, B. Johnson, R. Revadelo, G. Eifert, A. Cox, J. Beckett, T. Osborn, C. Thrasher, R. Lowe and D. Konkolewicz, 3D printable adhesive elastomers with dynamic covalent bond rearrangement, *Soft Matter*, 2023, **19**, 4964–4971, DOI: 10.1039/d3sm00394a.

23 M. Blanke, L. Postulka, I. Ciara, F. D'Acierno, M. Hildebrandt, J. S. Gutmann, R. Y. Dong, C. A. Michal and M. Giese, Manipulation of Liquid Crystalline Properties by Dynamic Covalent Chemistry–En Route to Adaptive Materials, *ACS Appl. Mater. Interfaces*, 2022, **14**, 16755–16763, DOI: 10.1021/acsami.2c03241.

24 M. Blanke, T. Neumann, M. E. Gutierrez Suburu, O. Prymak, C. Wölper, C. A. Strassert and M. Giese, Tuning the Fluorescence in Dynamic Covalent Bonded Liquid Crystals, *ACS Appl. Mater. Interfaces*, 2022, **14**, 55864–55872, DOI: 10.1021/acsami.2c16209.

25 H.-B. Bu, G. Götz, E. Reinold, A. Vogt, S. Schmid, R. Blanco, J. L. Segura and P. Bäuerle, Click-functionalization of conducting poly(3,4-ethylenedioxythiophene) (PEDOT), *Chem. Commun.*, 2008, 1320–1322, DOI: 10.1039/B718077B.

26 K. E. Feldman and D. C. Martin, Functional Conducting Polymers via Thiol-ene Chemistry, *Biosensors*, 2012, **2**, 305–317, DOI: 10.3390/bios2030305.

27 B. Wei, L. Ouyang, J. Liu and D. C. Martin, Post-polymerization functionalization of poly(3,4-propylenedioxythiophene) (PProDOT) via thiol-ene "click" chemistry, *J. Mater. Chem. B*, 2015, **3**, 5028–5034, DOI: 10.1039/C4TB02033B.

28 P. J. Molino, G. G. Wallace and T. W. Hanks, Hydrophobic conducting polymer films from post deposition thiol exposure, *Synth. Met.*, 2012, **162**, 1464–1470, DOI: 10.1016/j.synthmet.2012.06.013.

29 Y. Han, Y. Cao and H. Lei, Dynamic Covalent Hydrogels: Strong yet Dynamic, *Gels*, 2022, **8**, 577, DOI: 10.3390/gels8090577.

30 H. Lee, J. Kim, M. Lee and J. Kang, Dynamic Bond Chemistry in Soft Materials: Bridging Adaptability and Mechanical Robustness, *Chem. Rev.*, 2025, **125**, 11379–11425, DOI: 10.1021/acs.chemrev.5c00566.

31 Z. Q. Lei, P. Xie, M. Z. Rong and M. Q. Zhang, Catalyst-free dynamic exchange of aromatic Schiff base bonds and its application to self-healing and remolding of crosslinked polymers, *J. Mater. Chem. A*, 2015, **3**, 19662–19668, DOI: 10.1039/C5TA05788D.

32 G. Godeau, T. Darmanin and F. Guittard, Switchable surfaces from highly hydrophobic to highly hydrophilic using covalent imine bonds, *J. Appl. Polym. Sci.*, 2016, **133**, 43130, DOI: 10.1002/app.43130.

33 L. Carballido, T. Karbowiak and E. Bou-Maroun, Design and Synthesis Optimization of Fluorescent Acrylate-Based and Silicate-Based Materials for Carbonyl Adsorption, *Polymers*, 2025, **17**(13), 1843, DOI: 10.3390/polym17131843.

34 L. Wang, L. Wang, T. Xia, L. Dong, H. Chen and L. Li, Selective fluorescence determination of chromium(VI) with poly-4-vinylaninline nanoparticles, *Spectrochim. Acta, Part A*, 2004, **60**(11), 2465–2468, DOI: 10.1016/j.saa.2003.11.028.

35 J. H. Jin, J. M. An, D. Kim, S. Lee, M. Kim and D. Kim, Amino-SBBF (Single Benzene-based Fluorophore) Library: Its Synthesis, Photophysical Property, and Cellular Imaging Application, *Dyes Pigm.*, 2024, **221**, 111811, DOI: 10.1016/j.dyepig.2023.111811.

36 M. Shi, C. Xu, Z. Yang, L. Wang, S. Tan and G. Xu, Tuning of reversible thermochromic properties of salicylaldehyde Schiff bases through the substitution of methoxy and nitro groups, *J. Mol. Struct.*, 2019, **1182**, 72–78, DOI: 10.1016/j.molstruc.2019.01.012.

37 V. Madhura, M. V. Kulkarni, S. Badami, J. Yenagi and J. Tonannavar, Effect of nitro groups on the photo physical properties of benzimidazolone: a solvatochromic study, *Spectrochim. Acta, Part A*, 2011, **84**, 137–143, DOI: 10.1016/j.saa.2011.09.021.

38 F. Arenhart Soares, G. Martinez-Denegri, L. A. Baptista, P. Ślęczkowski and A. Steinbüchel, Balancing the Push–Pull Effect on the Synthesis and Fluorescent Properties of New ESIPT Dyes for Thin Film Applications, *J. Phys. Chem. C*, 2023, **127**, 17624–17636, DOI: 10.1021/acs.jpcc.3c04543.

39 O. Lange, A. Riabchunova, K. J. Haseloff, C. Kleeberg, M. Karnahl and S. Tschierlei, Push and Pull: the Impact of Amino and Nitro Substituents on Heteroleptic Cu(I) Photosensitizers, *Chemistry*, 2025, **31**, e202500583, DOI: 10.1002/chem.202500583.

40 A. Ullah, M. Ibrahim, A. Yousuf, M. A. Ali, H.-L. Xu and M. Arshad, Crafting optical wonders: The interplay of electron push–pull dynamics and π-conjugation in non–linear optics, *Next Mater.*, 2025, **9**, 101239, DOI: 10.1016/j.nxmate.2025.101239.

41 N. Yang, S. Zhang, Y. Cui, J. Wang, S. Cheng and J. Hou, Molecular design for low-cost organic photovoltaic materials, *Nat. Rev. Mater.*, 2025, **10**, 404–424, DOI: 10.1038/s41578-025-00792-4.

42 F. Della Sala and E. R. Kay, Reversible Control of Nanoparticle Functionalization and Physicochemical Properties by Dynamic Covalent Exchange, *Angew. Chem.*, 2015, **127**(14), 4261–4265, DOI: 10.1002/ange.201409602.

43 Y. Zhang, Y. Qi, S. Ulrich, M. Barboiu and O. Ramström, Dynamic Covalent Polymers for Biomedical Applications, *Mater. Chem. Front.*, 2020, **4**(2), 489–506, DOI: 10.1039/C9QM00598F.

44 E. Takács and L. Wojnárovits, Comparison of the reactivity of acrylate and methacrylate monomers, *Radiat. Phys. Chem.*, 1995, **46**(4–6), 1007–1010, DOI: 10.1016/0969-806X(95)00310-T.

45 M. Takagi, T. Shimazaki, O. Kobayashi, T. Ishimoto and M. Tachikawa, Theoretical and machine learning models for reaction-barrier predictions: acrylate and methacrylate radical reactions, *Phys. Chem. Chem. Phys.*, 2025, **27**(4), 1772–1777, DOI: 10.1039/d4cp04656k.

46 Y. Li, R. K. Kankala, L. Wu, A.-Z. Chen and S.-B. Wang, 3D-Printed Photocurable Resin with Synergistic Hydrogen Bonding Based on Deep Eutectic Solvent, *ACS Appl. Polym. Mater.*, 2023, **5**(1), 991–1001, DOI: 10.1021/acsapm.2c01916.

47 Y. Yue, J. Gu, J. Han, Q. Wu and J. Jiang, Effects of cellulose/salicylaldehyde thiosemicarbazone complexes on PVA based hydrogels: Portable, reusable, and high-precision luminescence sensing of Cu_2, *J. Hazard. Mater.*, 2021, **401**, 123798, DOI: 10.1016/j.jhazmat.2020.123798.